Available online at www.sciencedirect.com
SCIENCE DIRECT®
European Journal of Mechanics B/Fluids 23 (2004) 427–442

Temporal statistics in high Rayleigh number convective turbulence

R. Camussi [a,*], R. Verzicco [b]

[a] *Università Roma 'Tre', DIMI, Via della Vasca Navale 79, 00146 Roma, Italy*
[b] *Politecnico di Bari, DIMeG and CEMeC, Via Re David 200, 70125, Bari, Italy*

Received 25 February 2003; accepted 30 October 2003

Abstract

Temporal statistics of temperature and velocity fluctuations are studied in a highly turbulent convective flow developed within a cylindrical cell of aspect ratio $\Gamma = 1/2$. Numerical data are analyzed for Ra up to 2×10^{11} at fixed Prandtl number ($Pr = 0.7$). Temperature and velocity time series are collected from numerical probes placed within the fluid volume in the bulk and close to the boundaries. It is shown that the effects of the boundaries and of the large scale recirculation are reflected in the temporal statistics of the analyzed quantities. Spectra and structure functions show that the temperature statistics follow the Bolgiano scaling while the velocity fluctuations exhibit scaling laws which are surprisingly very close to those of the temperature. These results are in contrast with the Bolgiano or Kolmogorov behaviors expected for the velocity statistics and a possible theoretical explanation is presented.

1. Introduction

A physical model which is commonly adopted in experimental investigations of convective turbulence, is the buoyancy-driven motion developed within a closed container filled with fluid, and activated by a temperature difference Δ applied across the top and the bottom plates. The great interest manifested towards this physical problem (see, e.g., [1]) is motivated by the peculiarities of convective turbulence connected with the action of buoyancy forces. Indeed, in addition to geometrical parameters (such as the aspect ratio Γ defining the ratio between the lateral and vertical extent of the cell) the most important dimensionless group governing the convective turbulence is the Rayleigh number $Ra = g\alpha\Delta h^3/(\nu k)$ (h denotes the separation distance between the hot and cold plates, ν the kinematic viscosity, k the thermal diffusivity, α is the isobaric thermal expansion coefficient of the fluid and g the acceleration of gravity). For increasing Δ, buoyancy forces drive the fluid motion leading to the onset of spatio-temporal instabilities and, when Ra is sufficiently large, to turbulence. Other parameters of interest are the Prandtl number $Pr = \nu/k$ which accounts for the thermo-physical properties of the fluid, and the Nusselt number $Nu = Hh/(\lambda\Delta)$ (where H is the heat per unit surface transferred between the two plates and λ the fluid thermal conductivity), a dimensionless form of the heat transfer.

A key issue in the study of convective turbulence is to understand the way buoyancy forces and temperature influence the turbulence statistics. Buoyancy forces affect the large scale flow by the generation of convective rolls whose features depend both on the geometry of the cell (see, e.g., [2]) and on the Ra number (see, e.g., [3]). Small scales, or large frequency, statistics are also deeply influenced by buoyancy since, as pointed out by Aivalis et al. [4], the temperature is a dynamical variable which, under certain circumstances, plays the role of an active scalar. Different behaviors are indeed observed at different scales

* Corresponding author.
E-mail address: camussi@uniroma3.it (R. Camussi).

0997-7546/$ – see front matter
doi:10.1016/j.euromechflu.2003.10.012

depending on the relative importance of buoyancy and inertia forces and different dynamics controlling the energy cascade from large to small scales might occur. This behavior is manifested as different scaling laws in the temperature and velocity spectra which might coexist for different ranges of wavenumbers. The crossover scale between the buoyancy-driven and inertia-driven regimes is identified by the so called Bolgiano scale (see, e.g., [5]) which is defined as:

$$\mathcal{L}_B \simeq \frac{\bar{\varepsilon}^{5/4}}{(g\alpha)^{3/2}\overline{N}^{3/4}}, \tag{1}$$

where $\bar{\varepsilon}$ and $\overline{N}$ are, respectively, the averaged turbulent kinetic energy and temperature variance dissipation rates. As pointed out by Grossman and L'vov [6], at $Pr > 1$ the Bolgiano scale can be much smaller than the energy injection scale. For length scales larger than $\mathcal{L}_B$ a buoyancy driven regime is expected where the temperature spectrum decays with a $-7/5$ power law while velocity spectra exhibit a $-11/5$ power law (Bolgiano dynamics). For scales smaller than $\mathcal{L}_B$ inertia forces are expected to dominate and the classical Kolmogorov scaling [7,8] with $-5/3$ decay is expected to hold for the velocity. In this regime the temperature behaves like a passive scalar and the Kolmogorov scaling applies also for the temperature spectra. Theoretical studies (e.g., [9,10]) have shown that the Kolmogorov scaling corresponds to a constant energy flux towards the small scales while the Bolgiano scaling corresponds to a scale-independent entropy flux.

The above described physical picture is supported by several experimental results performed in the last few decades at very high Ra. Most of the experimental studies, however, were concerned with temperature statistics since the temperature T can be measured in a relatively easy manner. Temperature statistics have been analyzed both in terms of frequency spectra and, in the physical domain, in terms of the so called p-order temperature structure function, defined as:

$$S_T^p(\tau) = \left\langle \left[T(t+\tau) - T(t)\right]^p \right\rangle. \tag{2}$$

Limiting to large Pr number fluids ($Pr > 0.3$), temperature spectra obtained in gaseous and liquid helium and water have shown agreement with the Bolgiano scaling (e.g., [11–13]). The Bolgiano and the Kolmogorov regimes have been observed simultaneously in the temperature spectra also in a recent experiment by Niemela et al. [14]. Temperature structure functions evidencing the Bolgiano scaling have also been reported (see, e.g., the recent experiments by Aivalis et al. [4], and Skrbek et al. [15]). Fewer experimental results are concerned with the velocity statistics in view of the difficulties in measuring this quantity (see, e.g., [16]). Also in this case both energy spectra and velocity structure functions have been analyzed, the latter being defined as:

$$S_v^p(\tau) = \left\langle \left[v(t+\tau) - v(t)\right]^p \right\rangle, \tag{3}$$

where $v(t)$ denotes the measured velocity component. The Bolgiano scaling was observed in the experiment by Tong and Shen [17] using the photon-correlation homodyne spectroscopy technique in a $\Gamma \geqslant 1$ water filled cell. Velocity spectra obtained by Laser Doppler Velocimetry (LDV) technique in a $\Gamma = 0.7$ cell filled with SF_6 gas close to the critical point, were presented by Ashkenazi and Steinberg [18,19] showing the signature of the large scale recirculation cell and a good agreement with the $-11/5$ Bolgiano scaling. In this case however, the Pr number of the flow was very high ($Pr = 93$). More recently Shang and Xia [20] have shown, by LDV measurements in a $\Gamma = 1$ water filled cell, the existence of the Bolgiano scaling in the vertical velocity spectra but a surprising $-7/5$ scaling in the low frequency range was also reported.

The few and sometimes contradictory experimental results in high Ra convection at large Pr, highlights that a clear picture of the effect of buoyancy and temperature on the overall statistics is still far from clear. On the other hand, since the present numerical simulations have already been validated by cross-checks with other simulations and laboratory experiments available from the literature, we wish to compute some accurate velocity statistics in order to provide a frame for the interpretation of the latest results; this represents the main motivation for the present study. The configuration adopted and the numerical set-up is the same as reported in Verzicco and Camussi [3] and a brief description is given in Section 2. The statistical analysis is conducted by computing temporal frequency spectra, probability density functions (PDF) and structure functions of both the temperature and the three velocity components. The present analysis is an extension of previous studies presented in Verzicco and Camussi [3] where attention was focused mostly on the effect of the large-scale recirculation. The main results presently achieved are reported in Section 3 while final discussions and conclusions are given in Section 4.

2. The physical problem

Temperature and velocity data were obtained by a direct numerical simulation of the three-dimensional unsteady Navier–Stokes equations with the Boussinesq approximation. Details on the numerical set-up are given in Verzicco and Camussi [3]. The flow is enclosed in a cylindrical cell of aspect ratio $\Gamma = 1/2$ heated from below and cooled from above at $Pr = 0.7$. This configuration replicates the experimental set-ups of Chavanne et al. [21], Niemela et al. [14] and Roche et al. [22] who

performed the experiments using gaseous helium close to the critical point as working fluid. In the numerical simulation *Ra* is varied from 2×10^6 up to 2×10^{11} but the present analysis is mainly focused to the cases at $Ra = 2 \times 10^{10}$ and 2×10^{11}, where the *Ra* number is large enough for sufficiently broad scaling ranges to be visualized. For the present purposes, the main advantage of the numerical approach is the possibility of inserting within the fluid volume an arbitrary number of "ideal probes" which provide simultaneous point-wise measurements of temperature and of the three velocity components, without intrusivity problems. In the present analysis 400 probes are placed within the cell both in the bulk and close to the walls. 20 azimuthally equispaced probes are located on 20 circles 2 of which, containing 40 probes, are located close to the hot plate, 2 close to the cold plate, 9 halfway between the plates in the bulk and 1 halfway between the plates close to the sidewall. For a sketch of the probe positions inside the cell see Fig. 1 of Verzicco and Camussi [3]; here we only wish to stress that in the plate region, the minimum distance of the probes from the wall is $\Delta_z/h = 0.0052$ while viscous and thermal boundary layer thicknesses are, respectively, $\delta_v/h = 0.00876$ and $\delta_\theta/h = 0.00184$ at $Ra = 2 \times 10^{10}$ and $\delta_v/h = 0.00454$ and $\delta_\theta/h = 0.00110$ at $Ra = 2 \times 10^{11}$. This implies that the probes in the wall region are 'within' the viscous boundary layer but outside the thermal layer; nevertheless we will see that the flow dynamics in this region is strongly influenced by the wall and definitely different from the bulk region. The bulk region is tagged by the spatial measurements and averages of global quantities, such as $\bar{\varepsilon}$ and $\overline{N}$, already presented in Verzicco and Camussi [3] (see Fig. 19 of that paper). In the bulk region, owing to the large number of probes and the long flow evolution, about 220 large-eddy-turnover times at the highest *Ra*, about 2×10^7 samples have been collected while, according to the reduced number of available probes, the samples close to the walls are 'limited' to about 2×10^6. The analysis of high order statistics has been, therefore, limited to the bulk region. Similar limitations apply to the probes halfway between the plates and close to the sidewall; their distance from the wall is $\Delta_r/h = 0.09$ while the thickness of the lateral viscous boundary layer is $\delta_{lw}/h = 0.0242$ at $Ra = 2 \times 10^{10}$ and $\delta_{lw}/h = 0.0126$ at $Ra = 2 \times 10^{11}$; the probes are therefore outside the viscous boundary layer (the thermal boundary layer does not develop since the surface is perfectly adiabatic) even if, as in this case, the flow dynamics are affected by the wall.

We wish to stress that both spectra and structure functions are computed in the time domain. Indeed, except for regions of flow close to the hot/cold walls a mean velocity is not present thus it is not possible to apply the Taylor hypothesis to convert time to space. Furthermore, in the numerical simulation the governing equations have been made non-dimensional using the free-fall velocity $U = \sqrt{g\alpha\Delta h}$, the distance between hot and cold plates h and their temperature difference Δ, thus both the velocity components and the temperature as well as the statistical quantities associated with them are hereafter presented in non-dimensional form. Specifically, the non-dimensional temperature θ is defined as $\theta = (T - T_c)/\Delta$ so that $0 \leqslant \theta \leqslant 1$, with T_c the temperature of the cold plate.

3. Results

Examples of temperature and velocity spectra as well as second order structure functions were already presented in Verzicco and Camussi [3] but they are analyzed here in more detail. In the present approach we separate the results obtained close to the boundaries with respect to the statistical analysis in the bulk which, due to the larger number of samples available, is conducted more accurately.

3.1. Effect of the boundaries on the temperature and velocity statistics

The presence of the boundaries strongly affects the velocity and temperature statistics and different behaviors are observed depending on the flow region (i.e., close to the horizontal plates or to the lateral wall) as an effect of the large scale features. As noted in Verzicco and Camussi [3], at large *Ra* the dynamics in regions close to the horizontal plates are governed by the presence of a horizontal mean wind which (see also [23]), even if correlated to different large scale structures depending on the *Ra* magnitude, is always effective. However, such an effect does not seem to have a relevant influence on the temperature spectra. Indeed, as shown in Fig. 1, the temperature spectra obtained at $Ra = 2 \times 10^{10}$ and computed close to the lower and upper plates do not exhibit any scaling range. On the other hand, close to the lateral wall, a scaling range in the temperature spectra at $Ra = 2 \times 10^{10}$ is present (Fig. 2) and it appears close to the Kolmogorov $-5/3$ law. This seems to reflect the influence of the mean recirculation velocity which characterizes the temperature dynamics at this *Ra*.

Analogous results on the temperature spectra are obtained at $Ra = 2 \times 10^{11}$ and are reported in Fig. 3. As was shown in Verzicco and Camussi [3] at *Ra* larger than 2×10^{10} the large scale convective cell filling the whole volume breaks-up into two counter-rotating asymmetric unity-aspect-ratio rolls. This transition has an appreciable impact on the statistics of the bulk turbulence as well as close to the boundaries with the generation of a bump in the region of frequency or time scales which separates the power law range from the dissipation region. The presence of the bump, which produces the -1 slope, is documented close to the lateral wall, and it has been observed also experimentally in a similar flow (J. Niemela, personal communication). Kaneda et al. [26], in a recent high resolution DNS of homogeneous and isotropic turbulence, observed a bump

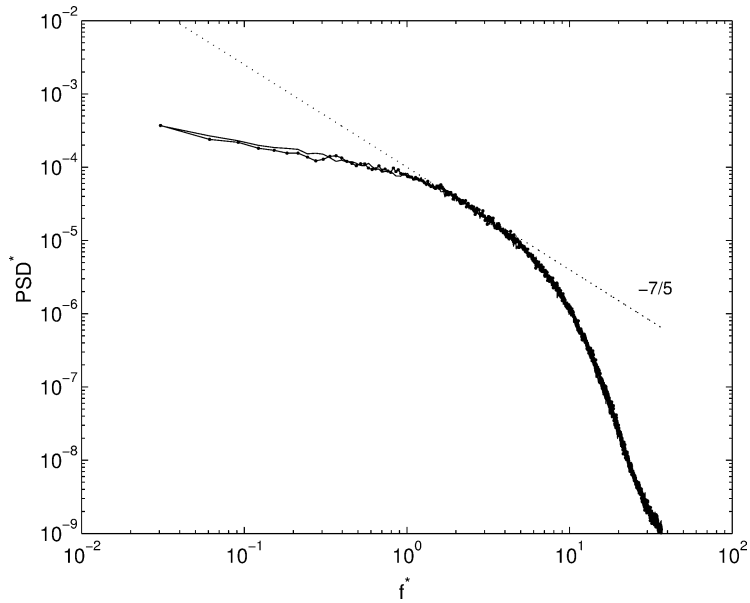

Fig. 1. Non-dimensional temperature frequency spectra computed close to the upper cold wall (solid line) and lower hot wall (solid-dot line) at $Ra = 2 \times 10^{10}$. The Bolgiano prediction is reported to show that no scaling range is observed. PSD^* and f^* denote non-dimensional quantities.

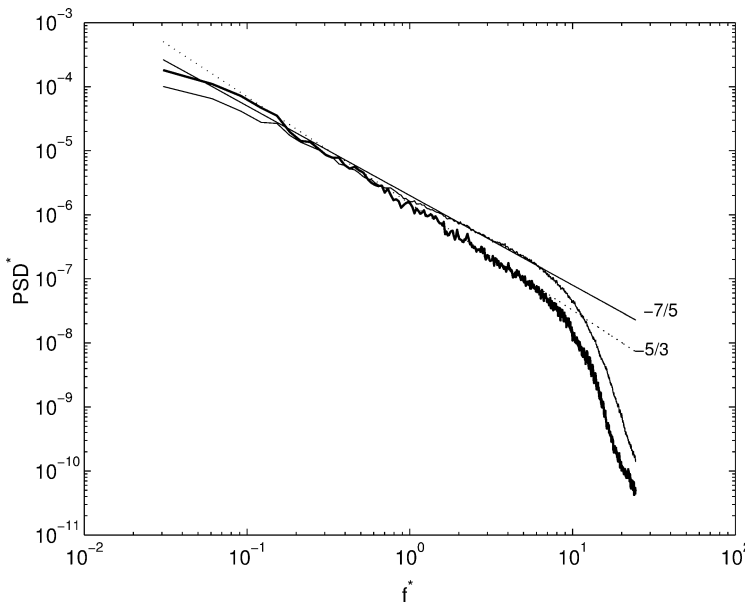

Fig. 2. Non-dimensional temperature frequency spectra computed close to the lateral wall (half height between the hot/cold walls) at $Ra = 2 \times 10^{10}$ (solid-bold line). The temperature spectrum obtained in the bulk is reported for comparison (solid line) as well as the Bolgiano (solid) and Kolmogorov (dotted) predictions.

in the velocity spectra at high frequencies. According to their analysis, the bump can be attributed to the different magnitude of the energy dissipation rate as compared to the kinetic energy flux. Present results seem to suggest that similar mechanisms should occur in convective turbulence. The direct computation of the temperature variance flux might help to clarify this point and further studies are needed to pursue this task.

The effect of *Ra* on the large scale features as well as the different dynamics observed close to the boundaries is documented also by the temperature PDFs which are reported in Fig. 4. PDFs of temperature fluctuations computed in the bulk exhibit clear exponential tails that enlarge for increasing *Ra*. At the hot (cold) plate the temperature PDFs are skewed towards positive

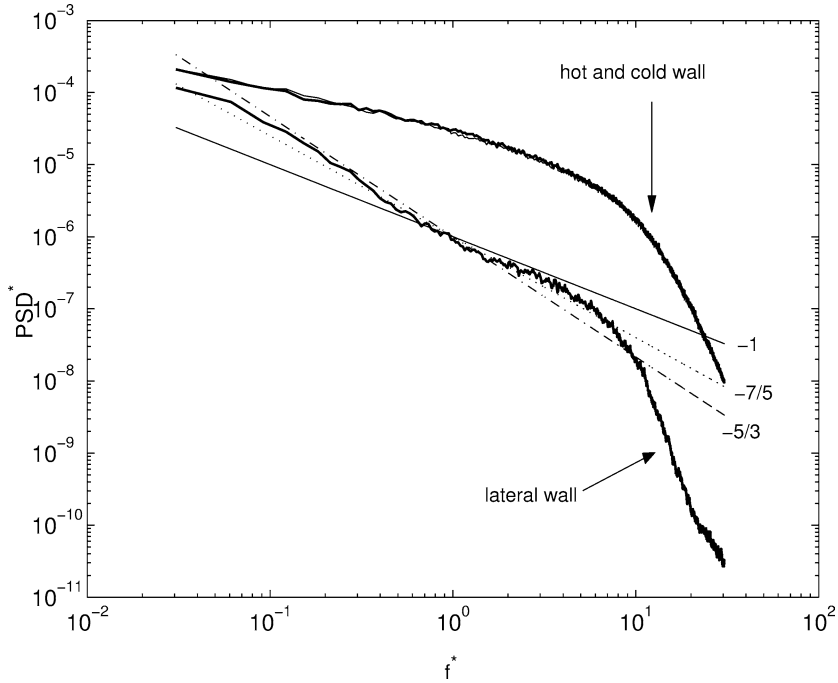

Fig. 3. Non-dimensional temperature frequency spectra at $Ra = 2 \times 10^{11}$ close to the boundaries.

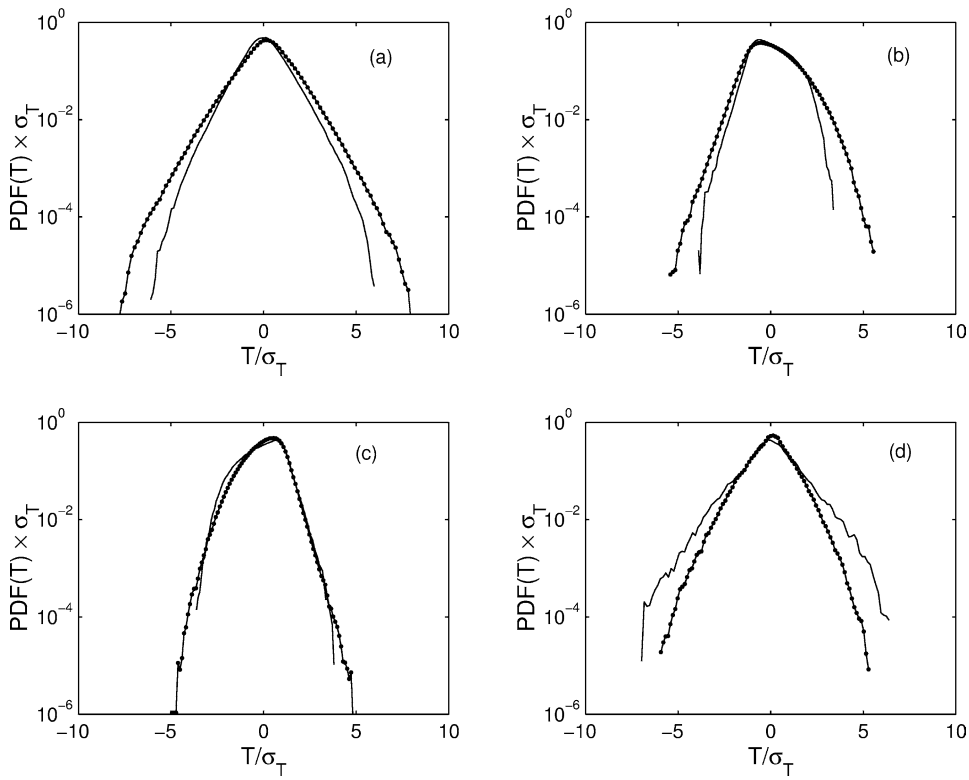

Fig. 4. Comparison between temperature PDF at $Ra = 2 \times 10^{11}$ (solid-dot) and $Ra = 2 \times 10^{10}$ (solid). (a) Bulk, (b) hot wall, (c) cold wall, (d) lateral wall.

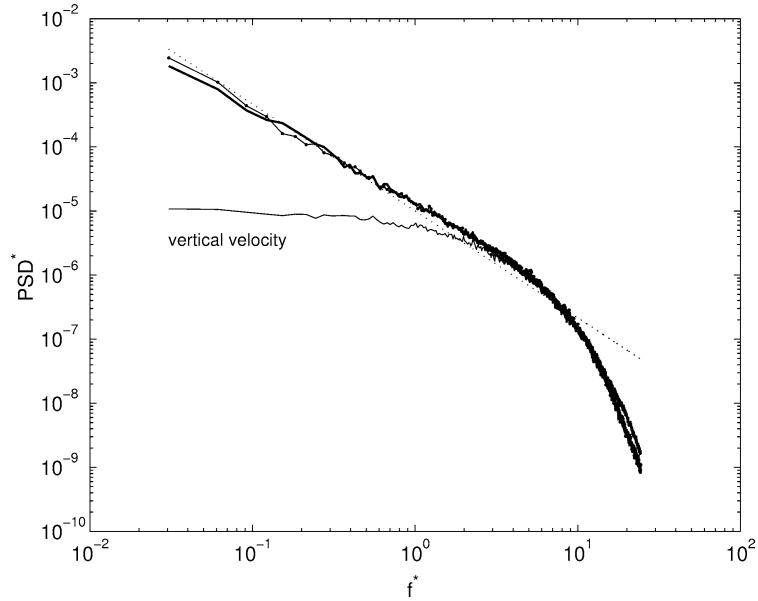

Fig. 5. Non-dimensional velocity frequency spectra computed close to the hot wall at $Ra = 2 \times 10^{10}$. Solid line is v_z, solid-bold line is v_θ, solid-dotted line is v_r. The dotted straight line is the Kolmogorov scaling ($f^{-5/3}$). The same result is obtained at the cold wall and is not reported for brevity.

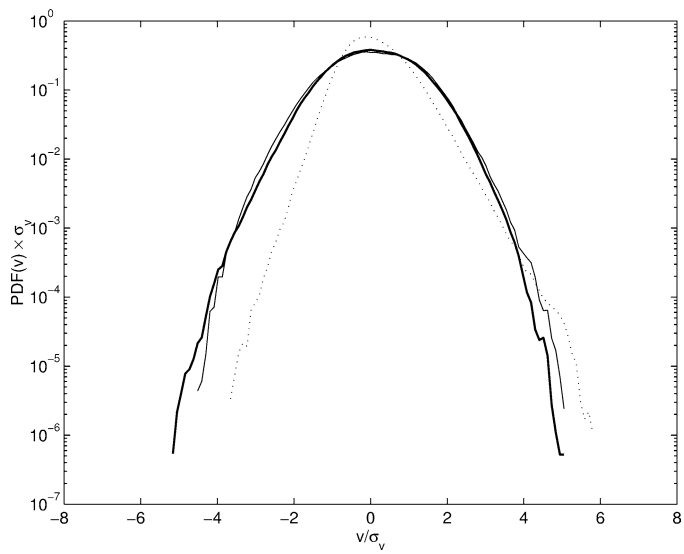

Fig. 6. Velocity PDFs close to the cold wall at $Ra = 2 \times 10^{11}$. Solid line is v_θ, solid-bold line is v_r, dotted line is v_z.

(negative) values thus showing in this case the strong influence of hot (cold) events which were not observed in the temperature spectra. Interesting features are observed close to the lateral wall where the PDFs' tails are larger at the lower *Ra* and are likely to be signatures of the diminished strength of the large scale convective roll.

The most relevant effect of the boundaries on the velocity spectra is the large scale anisotropy which, as shown in Figs. 5 and 8, significantly affects only the wall-normal of the three velocity components. Specifically, when close to the horizontal plates (Fig. 5) the low frequency range of the vertical velocity is lowered as an effect of the horizontal wind sweeping the plates that injects energy mainly on the horizontal velocity components. In spite of the temperature behavior reported in Fig. 1, the horizontal velocity is now sufficiently energetic to exhibit a scaling range which is close to the Kolmogorov $f^{-5/3}$ prediction. Similar results are obtained at the larger *Ra*.

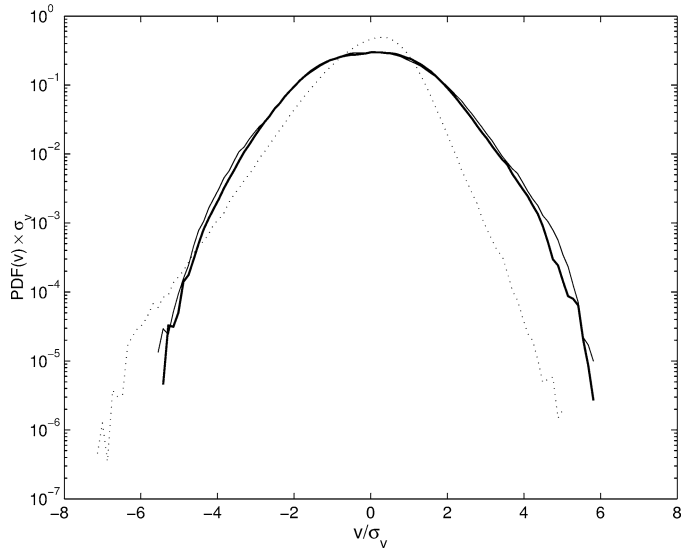

Fig. 7. Velocity PDFs close to the hot wall at $Ra = 2 \times 10^{11}$ (same symbols as in Fig. 6).

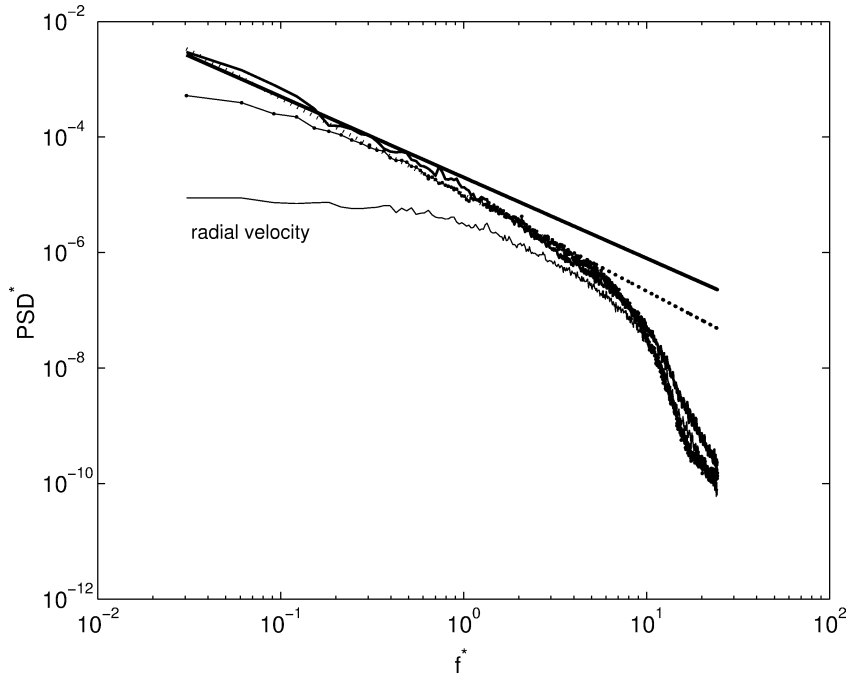

Fig. 8. Non-dimensional radial velocity frequency spectra computed close to the lateral wall at $Ra = 2 \times 10^{10}$. For line symbols see Fig. 5, solid straight line is the Bolgiano scaling of temperature ($f^{-7/5}$) while dotted straight line is the Kolmogorov scaling ($f^{-5/3}$).

The presence of hot/cold events affecting the temperature statistics close to the horizontal walls is reflected also in the velocity PDFs which are reported in Figs. 6 and 7. It is clear that the only component showing a strongly non-Gaussian statistic is the vertical one which develops strong positive or negative tails depending whether cold or hot events are statistically dominant.

In the vicinity of the lateral wall, the radial velocity component is inhibited and the same dynamics as close to the horizontal plates is observed with the radial velocity playing the role of the previously described vertical velocity component.

It is possible to conclude therefore that, accounting for the effects of the large scale features, the dynamics of both velocity and temperature close to the lateral wall at $Ra \geqslant 10^{10}$ is within the so-called inertia-driven regime since the Kolmogorov $f^{-5/3}$ scaling is consistently observed. Close to the horizontal plates the spectral features are dominated by the horizontal wind while

the signature of the hot/cold plumes is evidenced only by the PDFs. It is therefore evident that the events responsible for the hot/cold emission close to the horizontal walls are characterized by intermittent statistics which cannot be retrieved by the spectral analysis which projects the time signals over bases of trigonometric functions. The nature of such events can be studied in the time domain only by adopting some kind of conditional statistics which, taking advantage of the numerical simulation, can be coupled with direct visualizations of the 3D spatial velocity, temperature and vorticity fields close to the walls. This task is beyond the scope of the present paper and a study of these aspects is presently underway by the authors.

3.2. Statistics in the bulk

As was shown in Verzicco and Camussi [3], the temperature statistics in the bulk are characterized by Bolgiano dynamics which are manifested as a $-7/5$ slope in the scaling range of the spectra. For the sake of completeness, we report an example of such a result in Fig. 9 for the case at $Ra = 2 \times 10^{10}$. A similar behavior was observed also at *Ra* larger than 2×10^{10}.

Quite different behaviors are observed in the velocity statistics which surprisingly show results inconsistent with the scaling and statistics of the temperature and, in particular, with the expected Bolgiano dynamics. As a first indication, the velocity components PDF computed in the bulk are reported in Fig. 10. The deviations from the Gaussian curve are very small thus indicating that the velocity statistics are close to Gaussian in spite of the temperature PDF reported in Fig. 4. A similar result on the velocity statistics was reported by Ashkenazi and Steinberg [19] but it was ascribed to background noise effects in the experimental measurements.

Velocity spectra computed in the bulk at $Ra = 2 \times 10^{10}$ are reported in Fig. 11 in compensated form. It is clearly shown that even if a scaling range is present, the expected Bolgiano $-11/5$ law does not apply and even the Kolmogorov $-5/3$ decay seems too steep. The correct scaling law is surprisingly very close to that of the temperature spectra, that is $f^{-7/5}$. Analogous results are obtained at $Ra = 2 \times 10^{11}$ even if the scalings are less clear due to the presence of the bump which, as was shown in Verzicco and Camussi [3] strongly affects also the velocity statistics. At any rate, results reported in Fig. 12 clearly show that the Bolgiano scaling $-11/5$ is not observed while the Bolgiano scaling law of the temperature, $f^{-7/5}$, seems to be more appropriate also for the velocity spectra.

The scaling behaviors in the bulk are analyzed in more detail by the computation of the temperature and velocity structure functions. Results consistent with the Bolgiano scaling of temperature were presented in Verzicco and Camussi [3] in terms of second order temperature structure functions. Specifically, a 0.4 scaling exponent was observed in the temperature second

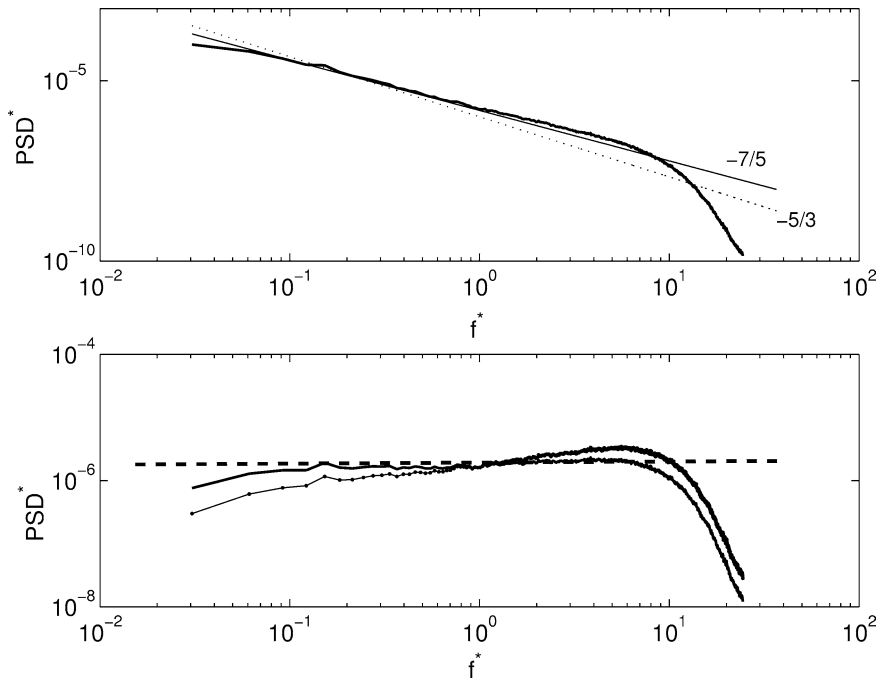

Fig. 9. Non-dimensional temperature frequency spectra computed in the bulk at $Ra = 2 \times 10^{10}$. The lower panel shows the compensated spectra (solid-bold line is $-7/5$ compensated, while solid-dot line is $-5/3$ compensated) evidencing the Bolgiano $-7/5$ scaling (dashed line is horizontal).

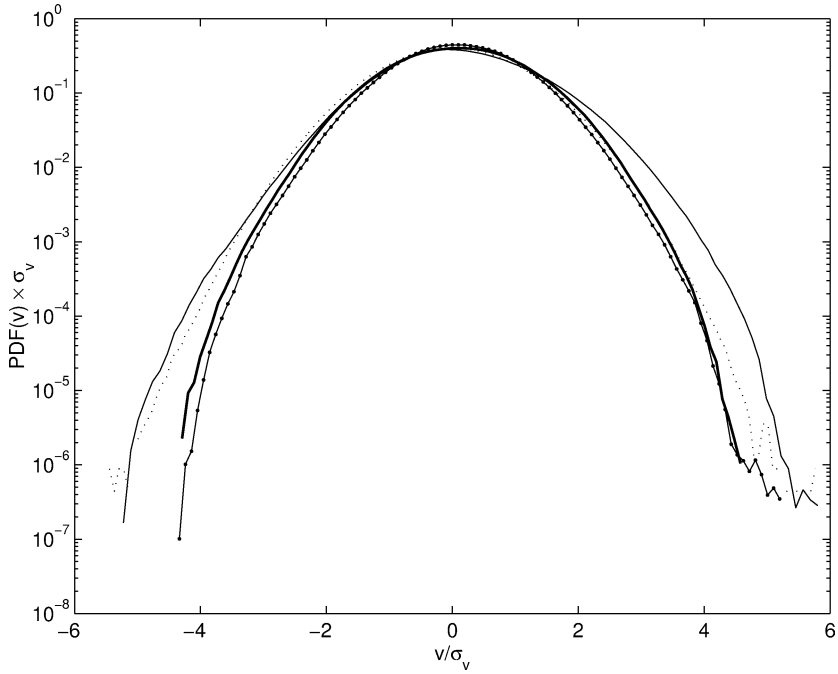

Fig. 10. Velocity PDF computed in the bulk at $Ra = 2 \times 10^{11}$. For symbols see caption of Fig. 6. Solid-dotted line represents a reference Gaussian curve. Analogous results are obtained at $Ra = 2 \times 10^{10}$ and are not reported for brevity.

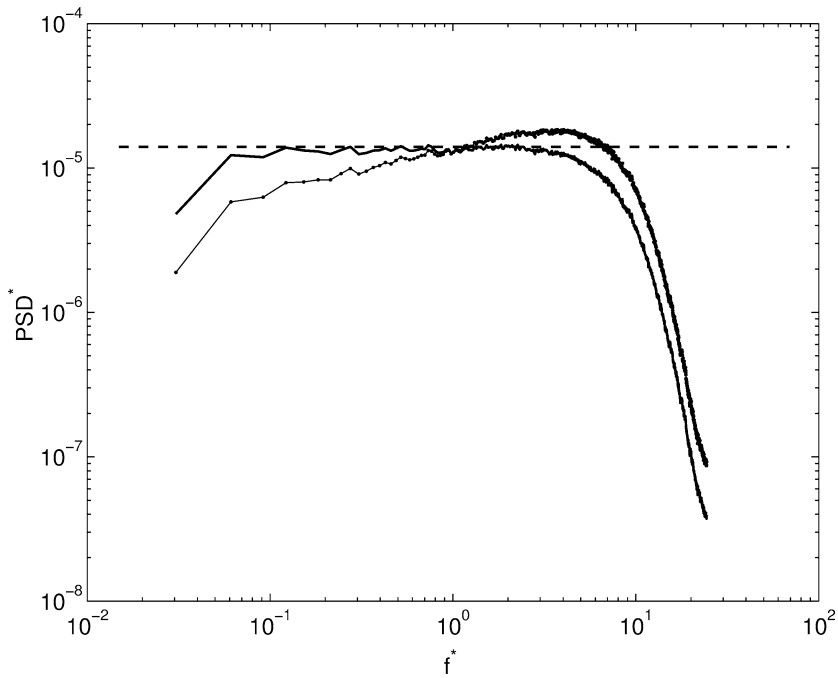

Fig. 11. Non-dimensional radial velocity frequency spectra computed in the bulk at $Ra = 2 \times 10^{10}$, compensated with respect to the Kolmogorov scaling $f^{-5/3}$ (solid-dot line) and the Bolgiano scaling $f^{-7/5}$ (solid-bold line) of the temperature.

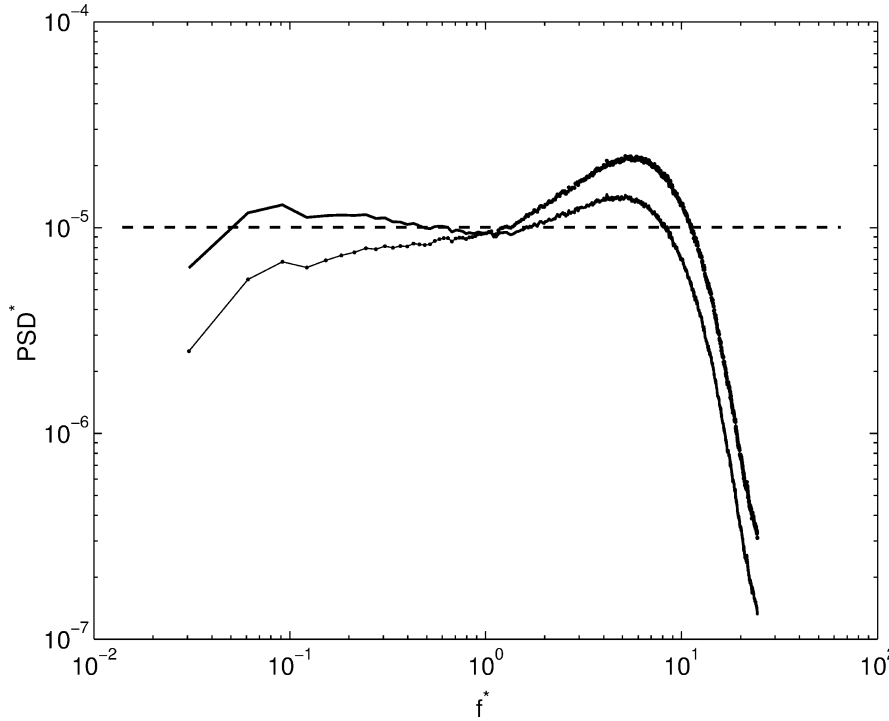

Fig. 12. Non-dimensional radial velocity frequency spectra computed in the bulk at $Ra = 2 \times 10^{11}$, compensated with respect to the Kolmogorov scaling and the Bolgiano scaling of the temperature (for symbols see Fig. 11).

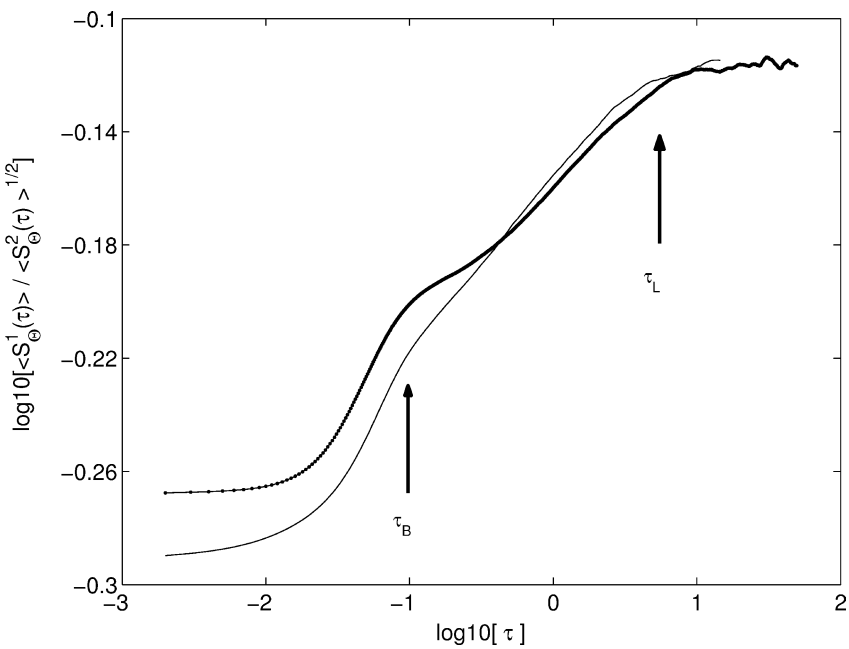

Fig. 13. Scaling of the normalized 1st order temperature structure function (following Ching [24]) computed in the bulk at $Ra = 2 \times 10^{10}$ (solid line) and $Ra = 2 \times 10^{11}$ (solid-dotted line). The time increment τ is non-dimensional and the approximated magnitude of the non-dimensional Bolgiano (τ_B) and integral (τ_L) time scales are also reported.

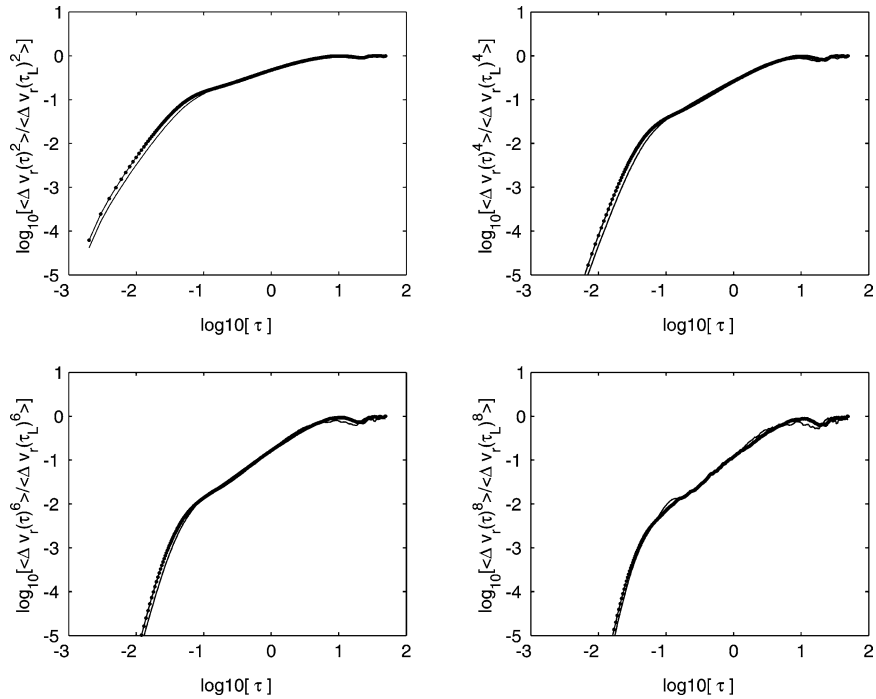

Fig. 14. Radial velocity structure functions computed in the bulk at $Ra = 2 \times 10^{10}$ (solid lines) and $Ra = 2 \times 10^{11}$ (solid-dotted lines). The structure functions are normalized with respect to the value assumed at the integral time scale τ_L.

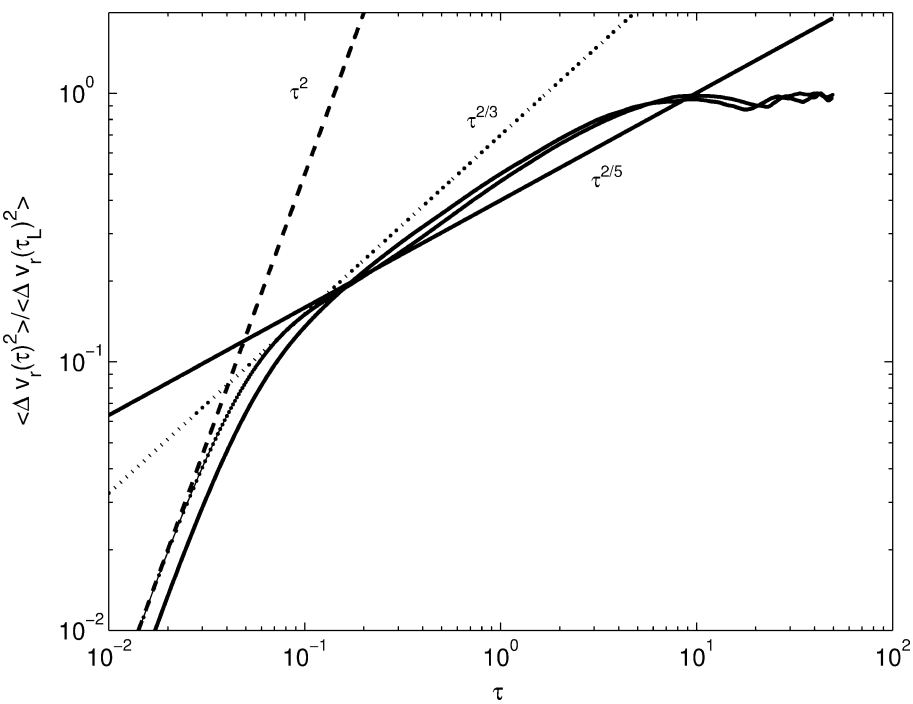

Fig. 15. Radial velocity second order structure functions (normalized as in Fig. 14) computed in the bulk at $Ra = 2 \times 10^{10}$ (solid line) and $Ra = 2 \times 10^{11}$ (solid-dotted line).

order structure functions in agreement with the $-7/5$ slope of the temperature spectra. Chavanne et al. [21], for flow conditions similar to the present ones, also observed a $-7/5$ slope in the spectra but their asymptotic scaling of the temperature second order structure functions was closer to $2/3$ rather than 0.4. Such a mismatch deserves further investigation.

According to Ching [24], the presence of a scaling region in the temperature fluctuations can be evidenced by a proper normalization of the first order temperature structure function which is reported in Fig. 13 as a function of the (non-dimensional) time increment. According to the approach usually adopted in experiments, the Bolgiano time-scale reported in this plot has been computed by the global estimation [24,13]:

$$\frac{\tau_B}{\tau_L} = \frac{\mathcal{L}_B}{h} = \frac{Nu^{1/2}}{(Ra\,Pr)^{1/4}}. \tag{4}$$

It is shown that a scaling range is observed for both *Ra* and for scales which are approximately included between the Bolgiano and the integral time scales, a result which is consistent with the temperature Bolgiano scalings above presented.

The scaling behavior evidenced by the velocity structure functions within the same range of time scales is instead quite different from the expected Bolgiano prediction which should lead, neglecting intermittency effects, to a scaling $\tau^{3p/5}$ for the p-order velocity structure functions. We point out that within the bulk the velocity fluctuation show good isotropy (see [3]) thus we limit ourselves to present the statistics of the radial velocity component. Examples of radial velocity structure functions are reported in Fig. 14 for $Ra = 2 \times 10^{10}$ and 2×10^{11}. This plot evidences that a scaling range is present and the scaling laws are not affected by *Ra*. In Fig. 14 moments up to the 8th order are presented, however, due to statistical convergence limitations, in the following the analysis is limited to moments order up to the 4th. This result induced us to analyze directly the scaling exponents, without adopting any relative scalings as in the ESS approach (see [25]) which, as shown by Aivalis et al. [4], might lead to unpredictable errors. Indeed, we wish to stress that we are not interested in determining accurately the scaling exponent's magnitude but our aim is to demonstrate the consistency of the spectral results in the physical domain. The second order velocity structure function is reported in detail in Fig. 15. Consistently with the velocity spectral analysis it is shown that the Bolgiano scaling expected for the velocity fluctuations is completely missed. The second order structure function shows an intermediate scaling between the Kolmogorov $2/3$ prediction and the temperature $2/5$ Bolgiano scaling.

This result is confirmed by the analysis of the local slope of the velocity structure functions computed by taking the derivative of the logarithm, and reported in Fig. 16. The agreement with the $p/5$ scaling is evident even though for $p > 6$ (results not reported for brevity) the presence of a scaling region is buried by large oscillations due to the lack of statistical convergence. To this extent it should be stressed that, as can be observed from Figs. 15 and 16, at small τ the p-order velocity structure functions follows the expected power law of the form τ^p. This result indicates that a statistical convergence at small time increment has been reached at least for $p \leqslant 4$.

In summary, the statistical analysis in the bulk shows that both spectra and velocity structure functions show scaling exponents close to those of the temperature, i.e., $-7/5$ for the spectra and $p/5$ for the structure functions. A similar scaling, even if coexisting with the Bolgiano $-11/5$ power law, was observed in the velocity spectra obtained experimentally by Shang and Xia [20]. The present results are surprising since neither the Kolmogorov scaling $-5/3$ nor the observed $-7/5$ scaling of the velocity spectra, are consistent with the scaling of the temperature. A summary of the results achieved in the bulk is given in Table 1 together with the expected Bolgiano scaling exponents.

In order for the present results to be interpreted, it is useful to work out the phenomenology and dimensional arguments leading to the Kolmogorov and Bolgiano scaling predictions. The first one should be achieved in the inertia-driven regime where the velocity difference at a time scale τ, denoted as u_τ, is driven by the rate of turbulent energy dissipation at the time scale τ, indicated as ε_τ. In this case $u_\tau \sim (\tau\varepsilon_\tau)^{1/3}$. The temperature behaves like a passive scalar, and, from dimensional arguments, the scaling of the temperature difference θ_τ should be $\theta_\tau \sim \varepsilon_\tau^{-1/6} N_\tau^{1/2} \tau^{1/3}$ where N_τ denotes the rate of temperature variance dissipation at the scale τ. In the buoyancy-driven regime the buoyancy force transforms the potential energy injected in the system into kinetic energy, therefore u_τ is generated by buoyancy and the scaling $u_\tau^2 \sim \alpha g \theta_\tau \tau$ should apply. This leads to the Bolgiano scaling of the temperature $\theta_\tau \sim N_\tau^{2/5} (\alpha g)^{-1/5} \tau^{1/5}$. In this regime the temperature is an active scalar and the scaling $u_\tau \sim \tau^{3/5}$ should apply for the velocity.

In contrast with the above arguments, in the present cases (see Table 1) it is observed that $\theta_\tau \sim \tau^{1/5}$ and $u_\tau \sim \tau^{1/5}$, that is $u_\tau \sim \theta_\tau$. Therefore the velocity scalings are likely to be driven by a different dynamics with respect to both the Kolmogorov and the Bolgiano ones. Basing on the observed phenomenology, what we can argue is that on one side the temperature dynamics is buoyancy dominated, on the other the velocity fluctuations are affected by both temperature variance and kinetic energy dissipation. Therefore both ε_τ and N_τ have to be accounted for to obtain a dimensional scaling of the velocity u_τ consistent with present results. From dimensional arguments it is in fact possible to retrieve the following relations:[1]

[1] The reported dimensional relationships are determined within a family of possible dimensional scalings which account for both ε_τ and N_τ. The choice presented is however the only one compatible with present observations.

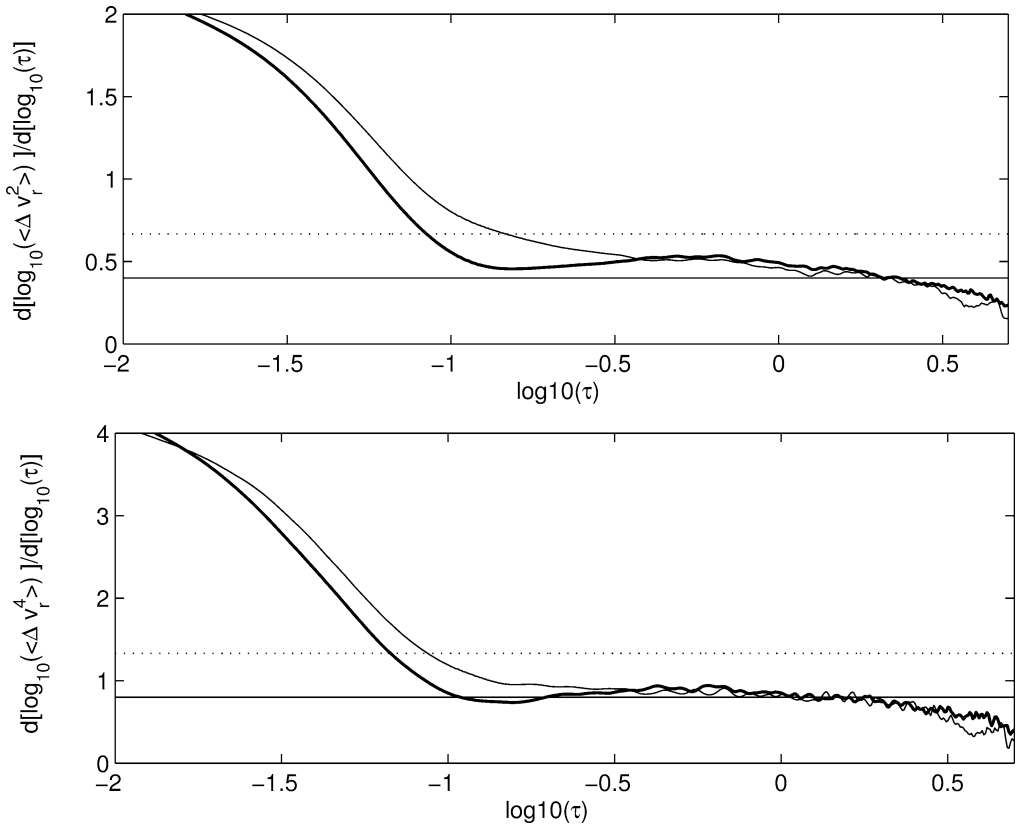

Fig. 16. Local slope of the radial velocity structure functions obtained from the logarithmic derivative. Structure functions are computed in the bulk at $Ra = 2 \times 10^{10}$ (solid lines) and $Ra = 2 \times 10^{11}$ (solid bold lines). The Bolgiano scaling expected for temperature (solid horizontal lines $= p/5$) and Kolmogorov scaling (dashed horizontal lines $= p/3$) are also reported.

Table 1
Scaling exponents obtained in the Bulk. Present results ('Obtained') are compared with those consistent with the Bolgiano scaling ('Bolgiano'). The main result is that the temperature satisfies the Bolgiano prediction while the velocity scaling exponents are the same as the temperature ones and are not consistent with the Bolgiano prediction. The scaling exponents are the same for the two *Ra* presently analyzed

	Temperature		Velocity	
	Bolgiano	Obtained	Bolgiano	Obtained
Spectra	$-7/5$	$-7/5$	$-11/5$	$-7/5$
Structure function	$p/5$	$p/5$	$3p/5$	$p/5$

$$\theta_\tau \sim N_\tau^{2/5} \tau^{1/5} \quad \text{(Buoyancy dominated)}, \tag{5}$$

$$u_\tau \sim \theta_\tau \varepsilon_\tau^{1/2} N_\tau^{-1/2} \quad \text{(Buoyancy + inertia)}. \tag{6}$$

Roughly speaking, what can be argued is that, according to the scenario proposed by Grossmann and Lohse [10], most of the thermal energy $\alpha g u \theta$ is put into the largest scales through the large scale convective rolls so that the remaining little thermal input is not dominant with respect to the inertial terms in the velocity dynamics. Temperature is active but not as strong as to induce a fully buoyancy-dominated regime in the velocity.

The above arguments can be checked in a rather simple, although somewhat naive, manner by taking into account the following exact global relations:

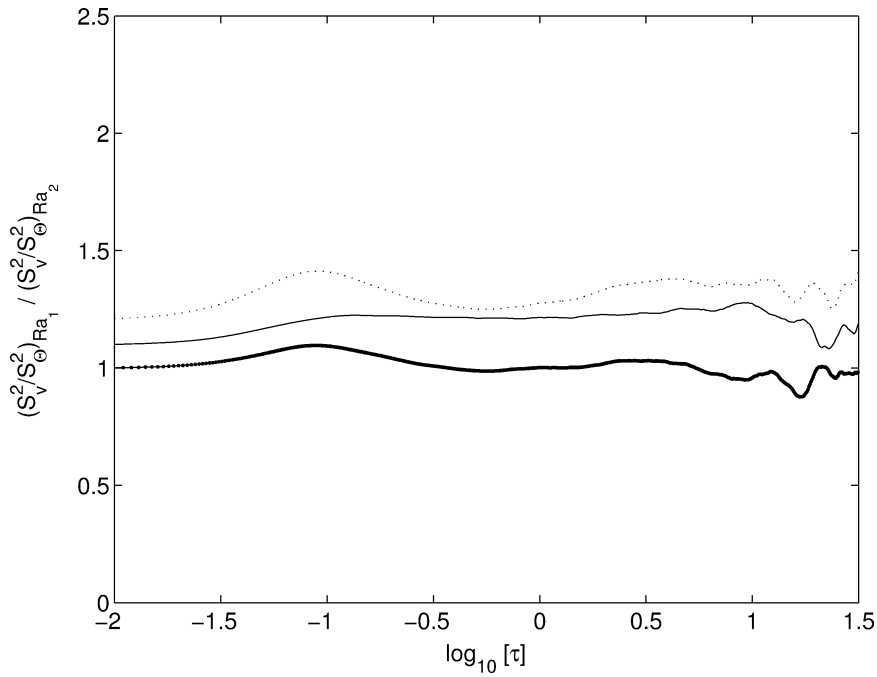

Fig. 17. Ratio between the quantity defined in Eq. (10) computed at different *Ra*. Dotted line is Eq. (10) computed at $Ra = 2 \times 10^{11}$ divided by the same quantity at $Ra = 2 \times 10^{9}$. Solid line is Eq. (10) computed at $Ra = 2 \times 10^{11}$ divided by the same quantity at $Ra = 2 \times 10^{10}$. Solid-dot line is Eq. (10) computed at $Ra = 2 \times 10^{10}$ divided by the same quantity at $Ra = 2 \times 10^{9}$.

$$\bar{\varepsilon} = \frac{Nu - 1}{\sqrt{Ra\,Pr}}, \tag{7}$$

$$\overline{N} = \frac{Nu}{\sqrt{Ra\,Pr}}. \tag{8}$$

Taking the average of the square of Eq. (6) without accounting for intermittency effects and assuming ε_τ and N_τ to be statistically independent, the following result should apply:

$$\langle u_\tau^2 \rangle \sim \langle \theta_\tau^2 \rangle \frac{Nu - 1}{Nu} \tag{9}$$

and at sufficiently high *Ra* (where $Nu \approx Nu - 1$)

$$\frac{\langle u_\tau^2 \rangle}{\langle \theta_\tau^2 \rangle} \sim const. \tag{10}$$

Relation (10) indicates that the ratio between the second order temperature and velocity structure functions should be independent of τ. Furthermore, the derivation of relation (9) from Eq. (6) should be verified by checking that the ratio of Eq. (10) is independent of *Ra* too.

These arguments can be easily checked from present data and an example is reported in Fig. 17. Here the ratio of the quantities $\langle u_\tau^2 \rangle / \langle \theta_\tau^2 \rangle$ obtained at different *Ra* is computed. The ratios are reasonably of the order of unity, especially considering consecutive *Ra*, and within the range of time scales where the scaling relations apply. This result confirms that the ratio reported in Eq. (6) is independent of *Ra*. Furthermore, the quantities reported appear to be independent also of τ thus supporting the idea that relation (6) is consistent. The observed discrepancies might also be ascribed to the intermittency effects which are known to be different for the velocity and the temperature fluctuations (see, e.g., [15]).

4. Conclusions

Numerical time series obtained from a direct numerical simulation of a fully turbulent convective flow in a cylindrical cell at $Pr = 0.7$ have been analyzed for high *Ra* numbers (2×10^{10} and 2×10^{11}). The statistical indicators analyzed consisted

of temperature and velocity spectra, PDFs and structure functions. It is shown that the effect of the boundaries as well as of the large scale recirculations is reflected in the statistics of both velocity and temperature in the bulk and close to the walls. Different behaviors and anomalous dynamics are indeed observed depending on the region of fluid considered.

In the vicinity of the hot and cold horizontal plates, the detachment of hot or cold (presumed) plumes is not visualized by the spectra but it is evident from both the temperature and the vertical velocity PDFs. In this region the horizontal wind sweeping the plates does not influence the temperature which is damped by the boundary layer effects while the horizontal velocity components exhibit a Kolmogorov scaling. On the other hand, in the region of fluid close to the lateral wall a Kolmogorov $f^{-5/3}$ scaling is observed both in the velocity and in the temperature spectra. This result seems to indicate that the inertia-driven regime is prevalent in the volume of fluid close to the lateral wall.

The statistics in the bulk reveal that the temperature is driven by the Bolgiano dynamics since a $f^{-7/5}$ scaling is clearly observed in the spectra and the scaling $\tau^{2/5}$ in the second order structure functions (presented in Verzicco and Camussi [3]). However, the velocity fluctuations show dynamical features which are not consistent with the expected Bolgiano scaling. The scaling exponents of the velocity spectra and velocity structure functions are indeed very close to those of the temperature. A possible interpretation has been given, according to Grossmann and Lohse [10] and based on a dimensional reasoning, which accounts for both kinetic energy and temperature variance dissipation rates. However a clear physical picture is not found on account of the experimental results which only partially agree with our findings. Further analyses are needed to clarify the physical behavior behind the observed scalings, in particular by analyzing *Ra* larger than those available from the numerical simulation. To this extent, further theoretical analyses and experimental studies providing simultaneous measurements of temperature and velocity, are surely needed.

Acknowledgements

The simulation at the highest Rayleigh was possible thanks to the computer facilities of CASPUR (Consorzio interuniversitario per le Applicazioni di Supercalcolo Per Università e Ricerca). Drs. F. Massaioli and G. Amati are gratefully acknowledged for the technical support in implementing openMP and using parallel computers.

References

[1] E.D. Siggia, High Rayleigh number convection, Annu. Rev. Fluid Mech. 26 (1994) 137–168.
[2] Z.A. Daya, R.E. Ecke, Does turbulent convection feel the shape of the container? Phys. Rev. Lett. 87 (2001) 184501.
[3] R. Verzicco, R. Camussi, Numerical experiments on strongly turbulent thermal convection in a slender cylindrical cell, J. Fluid Mech. 477 (2003) 19–49.
[4] K.G. Aivalis, K.R. Sreenivasan, Y. Tsuji, J.C. Klewicki, C.A. Biltoft, Temperature structure functions for air flow over moderately heated ground, Phys. Fluids 14 (2002) 2439–2446.
[5] A.S. Monin, A.M. Yaglom, Statistical Fluid Mechanics, Vol. 2, MIT Press, 1975.
[6] S. Grossman, V.S. L'vov, Crossover of spectral scaling in thermal turbulence, Phys. Rev. E 47 (1993) 4161–4168.
[7] A.N. Kolmogorov, The local structure of turbulence in incompressible viscous fluid for very large Reynolds numbers, C. R. Akad. Sci. SSSR 30 (1941) 301–305.
[8] A.M. Obukov, Some specific features of atmospheric turbulence, J. Fluid Mech. 13 (1962) 77–81.
[9] V.S. L'vov, Spectra of velocity and temperature fluctuations with constant entropy flux of fully developed free-convective turbulence, Phys. Rev. Lett. 67 (1991) 687–690.
[10] S. Grossmann, D. Lohse, Fourier-Weierstrass mode analysis for thermally driven turbulence, Phys. Rev. Lett. 67 (1991) 445–448.
[11] B. Castaing, G. Gunaratne, F. Heslot, L. Kadanoff, A. Libchaber, S. Thomae, X.Z. Wu, S. Zaleski, G. Zanetti, Scaling of hard thermal turbulence in Rayleigh–Bénard convection, J. Fluid Mech. 204 (1989) 1–30.
[12] X.Z. Wu, L. Kadanoff, A. Libchaber, M. Sano, Frequency power spectrum of temperature fluctuations in free convection, Phys. Rev. Lett. 18 (1990) 2140–2143.
[13] F. Chillá, S. Ciliberto, C. Innocenti, E. Pampaloni, Boundary Layer and scaling properties in turbulent thermal convection, Nuovo Cimento D 15 (9) (1993) 1229–1249.
[14] J.J. Niemela, L. Skrbek, R.R. Sreenivasan, R.J. Donnely, Turbulent convection at very high Rayleigh numbers, Nature 404 (2000) 837–841.
[15] L. Skrbek, J.J. Niemela, K.R. Sreenivasan, R.J. Donnely, Temperature structure functions in the Bolgiano regime of thermal convection, Phys. Rev. E 66 (2002) 036303.
[16] Y. Shen, K.Q. Xia, P. Tong, Measured local velocity fluctuations in turbulent convection, Phys. Rev. Lett. 75 (1995) 437–440.
[17] P. Tong, Y. Shen, Relative velocity fluctuations in turbulent Rayleigh–Bènard convection, Phys. Rev. Lett. 69 (1992) 2066–2069.
[18] S. Ashkenazi, V. Steinberg, High Rayleigh number turbulent convection in a gas near the gas–liquid critical point, Phys. Rev. Lett. 83 (1999) 3641–3644.
[19] S. Ashkenazi, V. Steinberg, Spectra and statistics of velocity and temperature fluctuations in turbulent convection, Phys. Rev. Lett. 83 (1999) 4760–4763.

[20] X.D. Shang, K.Q. Xia, Scaling of the velocity power spectra in turbulent thermal convection, Phys. Rev. E 64 (2001) 065301.
[21] X. Chavanne, F. Chillà, B. Chabaud, B. Castaing, B. Hebral, Turbulent Rayleigh–Bénard convection in gaseous and liquid He, Phys. Fluids 13 (2001) 1300–1320.
[22] P.E. Roche, B. Castaing, B. Chabaud, B. Hebral, Observation of the $1/2$ power law in Rayleigh–Bénard convection, Phys. Rev. E 63 (2001) 045303.
[23] S. Grossmann, D. Lohse, Scaling in thermal convection: a unifying theory, J. Fluid Mech. 407 (2000) 27–56.
[24] E.S.C. Ching, Intermittency of temperature field in turbulent convection, Phys. Rev. E 61 (2000) R33–R36.
[25] R. Benzi, S. Ciliberto, R. Tripiccione, C. Baudet, F. Massaioli, S. Succi, Extended self-similarity in turbulent flows, Phys. Rev. E 48 (1993) R29–R32.
[26] Y. Kaneda, T. Ishihara, M. Yokokawa, K. Itakura, A. Uno, Energy dissipation rate and energy spectrum in high resolution direct numerical simulations of turbulence in a periodic box, Phys. Fluids 15 (2003) L21–L24.